



HAL
open science

The Dichotomy of Mn–H Bond Cleavage and Kinetic Hydricity of Tricarbonyl Manganese Hydride Complexes

Elena S Osipova, Sergey A Kovalenko, Ekaterina S Gulyaeva, Nikolay V Kireev, Alexander A Pavlov, Oleg A Filippov, Anastasia A Danshina, Dmitry A Valyaev, Yves Canac, Elena S Shubina, et al.

► **To cite this version:**

Elena S Osipova, Sergey A Kovalenko, Ekaterina S Gulyaeva, Nikolay V Kireev, Alexander A Pavlov, et al.. The Dichotomy of Mn–H Bond Cleavage and Kinetic Hydricity of Tricarbonyl Manganese Hydride Complexes. *Molecules*, 2023, 28 (8), pp.3368. 10.3390/molecules28083368 . hal-04073711

HAL Id: hal-04073711

<https://hal.science/hal-04073711>

Submitted on 19 Apr 2023

HAL is a multi-disciplinary open access archive for the deposit and dissemination of scientific research documents, whether they are published or not. The documents may come from teaching and research institutions in France or abroad, or from public or private research centers.

L'archive ouverte pluridisciplinaire **HAL**, est destinée au dépôt et à la diffusion de documents scientifiques de niveau recherche, publiés ou non, émanant des établissements d'enseignement et de recherche français ou étrangers, des laboratoires publics ou privés.



Distributed under a Creative Commons Attribution 4.0 International License

Article

The Dichotomy of Mn–H Bond Cleavage and Kinetic Hydricity of Tricarbonyl Manganese Hydride Complexes

 Elena S. Osipova ¹, Sergey A. Kovalenko ¹, Ekaterina S. Gulyaeva ^{1,2}, Nikolay V. Kireev ¹, Alexander A. Pavlov ^{1,3}, Oleg A. Filippov ¹, Anastasia A. Danshina ^{1,4}, Dmitry A. Valyaev ^{2,*}, Yves Canac ², Elena S. Shubina ¹ and Natalia V. Belkova ^{1,*}

¹ A.N. Nesmeyanov Institute of Organoelement Compounds, Russian Academy of Sciences (INEOS RAS), 28, Vavilova Str., 119334 Moscow, Russia; aosipova92@gmail.com (E.S.O.); kovalenko2000as@gmail.com (S.A.K.); elenor.kagami@gmail.com (E.S.G.); koly-100@mail.ru (N.V.K.); alex90pavlov@mail.ru (A.A.P.); h-bond@ineos.ac.ru (O.A.F.); danshina.aa@phystech.edu (A.A.D.); shu@ineos.ac.ru (E.S.S.)

² LCC-CNRS, Université de Toulouse, CNRS, 205 Route de Narbonne, CEDEX 4, 31077 Toulouse, France; yves.canac@lcc-toulouse.fr

³ Center of National Technological Initiative, Bauman Moscow State Technical University, 2nd Baumanskaya Str., 5, Moscow, Russia

⁴ Moscow Institute of Physics and Technology (National Research University), Institutskiy per., 9, 141700 Dolgoprudny, Moscow Region, Russia

* Correspondence: dmitry.valyaev@lcc-toulouse.fr (D.A.V.); nataliabelk@ineos.ac.ru (N.V.B.)

Abstract: Acid-base characteristics (acidity, pK_a, and hydricity, ΔG[°]_H or k_H) of metal hydride complexes could be a helpful value for forecasting their activity in various catalytic reactions. Polarity of the M–H bond may change radically at the stage of formation of a non-covalent adduct with an acidic/basic partner. This stage is responsible for subsequent hydrogen ion (hydride or proton) transfer. Here, the reaction of tricarbonyl manganese hydrides *mer,trans*-[L₂Mn(CO)₃H] (**1**; L = P(OPh)₃, **2**; L = PPh₃) and *fac*-[(L-L')Mn(CO)₃H] (**3**, L-L' = Ph₂PCH₂PPh₂ (dppm); **4**, L-L' = Ph₂PCH₂-NHC) with organic bases and Lewis acid (B(C₆F₅)₃) was explored by spectroscopic (IR, NMR) methods to find the conditions for the Mn–H bond repolarization. Complex **1**, bearing phosphite ligands, features acidic properties (pK_a 21.3) but can serve also as a hydride donor (ΔG[‡]_{298K} = 19.8 kcal/mol). Complex **3** with pronounced hydride character can be deprotonated with KHMDS at the CH₂-bridge position in THF and at the Mn–H position in MeCN. The kinetic hydricity of manganese complexes **1–4** increases in the order *mer,trans*-[(P(OPh)₃)₂Mn(CO)₃H] (**1**) < *mer,trans*-[(PPh₃)₂Mn(CO)₃H] (**2**) ≈ *fac*-[(dppm)Mn(CO)₃H] (**3**) < *fac*-[(Ph₂PCH₂NHC)Mn(CO)₃H] (**4**), corresponding to the gain of the phosphorus ligand electron-donor properties.

Keywords: manganese hydrides; hydrogen bond; non-covalent interactions; proton and hydride transfer; hydricity

Citation: Osipova, E.S.; Kovalenko, S.A.; Gulyaeva, E.S.; Kireev, N.V.; Pavlov, A.A.; Filippov, O.A.; Danshina, A.A.; Valyaev, D.A.; Canac, Y.; Shubina, E.S.; et al. The Dichotomy of Mn–H Bond Cleavage and Kinetic Hydricity of Tricarbonyl Manganese Hydride Complexes. *Molecules* **2023**, *28*, x. <https://doi.org/10.3390/xxxxx>

Academic Editor: Zi-Jian Yao

Received: 16 March 2023

Revised: 04 April 2023

Accepted: 08 April 2023

Published: date



Copyright: © 2023 by the authors. Submitted for possible open access publication under the terms and conditions of the Creative Commons Attribution (CC BY) license (<https://creativecommons.org/licenses/by/4.0/>).

1. Introduction

A search for inexpensive and efficient catalysts that give more sustainable alternatives to platinum group metals recently led to remarkable progress in the development of catalytic systems based on organometallic manganese complexes [1,2]. While pincer-type Mn(I) derivatives still dominate in the field of catalytic (de)hydrogenation, it was demonstrated that less elaborated bidentate systems *fac*-[(L-L')Mn(CO)₃Br] may also be highly efficient [3]. Generally, the formation of catalytically relevant transition metal hydrides from the corresponding bromide precursors proceeds in situ in the presence of various basic additives. This activation step can be nicely illustrated for Mn(I) complexes *fac*-[(P-NHC)Mn(CO)₃Br] (P-NHC = κ²P,C-Ph₂PCH₂-NHC) [4] and *fac*-[(dppm^R)Mn(CO)₃Br] (dppm = κ²P,P-Ph₂PCH(R)PPh₂, R = H, Me, Ph) [5] in the presence of KHMDS leading to

the formation of cyclometalated species capable of activating dihydrogen via unconventional metal-ligand cooperation. The resulting hydride products *fac*-[(L-L')Mn(CO)₃H] interact with organic substrates to form non-covalent adducts and typically the formation of such intermediates directly precedes hydride/proton transfer steps providing *in fine* the hydrogenation of polar C=X bonds.

It is generally accepted that transition metal hydrides can be proton, hydride or hydrogen atom donors [6–8]. However, the vast majority of hydride complexes exhibit only one reactivity mode being determined by the nature of auxiliary ligands and relative charge on the core metal atom [9]. Nevertheless, there are a few families of hydrides in which the same hydride complex possesses distinct reactivity. *Dual* reactivity is well documented, for example, for groups 6–8 metal complexes [CpM(CO)₃H] (M = Mo, W), [(CO)₅MH] (M = Mn, Re) and [CpM(CO)₂H] (M = Fe, Ru, Os) [8,10–12]. Whether the M–H bond releases a proton or hydride, obviously, depends on the partner reagent. We have shown for the first time that the M–H bond polarity gets adjusted at the stage of a non-covalent complex formation preceding the M–H bond dissociation [13] (Scheme 1).

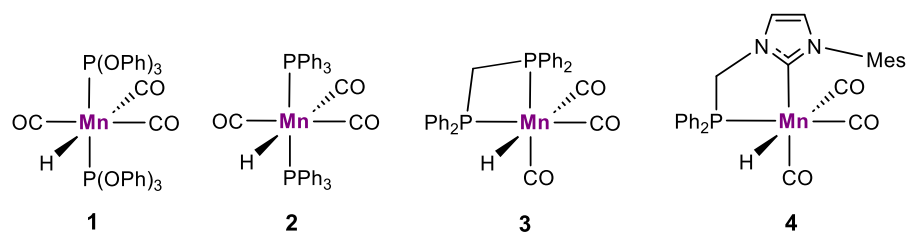


Scheme 1. LB = Lewis base, LA = Lewis acid.

The acidity and hydricity of the M–H bond can be quantified in terms of $\text{p}K_a$ and ΔG_{H^-} , respectively [14–16]. The quantitative scale of kinetic hydricity (k_{H^-}) has been developed for group 6–7 metal hydrides in the pioneering work of Bullock [11]. However, the data for manganese complexes are still scarce despite their utility as potential catalysts. Experimental values of acidity and hydricity are known only for [(CO)₅MnH] ($\text{p}K_a = 14.2$ in MeCN [8], $\Delta G_{\text{H}^-} = 59.61$ kcal/mol [17], $k_{\text{H}^-} = 50 \text{ M}^{-1}\text{s}^{-1}$ [11]), [(CO)₄(C₆H₆)MnH] ($\text{p}K_a = 26.8$ in MeCN [8]) and *cis*-[(CO)₄(PPh₃)MnH] ($\text{p}K_a = 20.4$ in MeCN [8], $k_{\text{H}^-} = 230 \text{ M}^{-1}\text{s}^{-1}$ [11]). There is a sole theoretical work devoted to a systematic study of (CO)₅MnH and (CO)_{5-n}(PH₃)_nMnH complexes [17] demonstrating that the hydricity of the metal hydride bond is greatly amplified when the CO ligand is replaced by a phosphine donor [17].

The research presented herein explores the dichotomy of Mn–H bond cleavage and the potential of its repolarization entailed by intermolecular interactions with Lewis acids and bases. By gaining an understanding of the acid-base characteristics of different manganese hydrides, it should be possible to forecast their catalytic performance and drive the catalyst design.

In this context, we chose two types of octahedral Mn(I) hydride complexes (Scheme 2) in which the Mn–H bond is expected to have different polarity. Electron-deficient phosphite ligands in complex *mer,trans*-[(P(OPh)₃)₂Mn(CO)₃H] (**1**) and more donating triarylphosphines in complex *mer,trans*-[(PPh₃)₂Mn(CO)₃H] (**2**) should provide them an acidic and basic character, respectively. In agreement with our expectations, complex **1** can be deprotonated by *t*BuOK [18], and complex **2** exhibits typical reactivity of “hydridic” hydride releasing H₂ [19,20] upon protonation by HBF₄·Et₂O [21]. The incorporation of chelating and more electron-rich ligands such as bidentate phosphine in *fac*-[(dppm)Mn(CO)₃H] (**3**) or phosphine-N-Heterocyclic carbene in *fac*-[(P-NHC)Mn(CO)₃H] (**4**) ought to increase the Mn–H basicity and hydride donating ability (Scheme 2). The acidity and hydricity of **1–4** have not been evaluated before this work; therefore, the entire set of these complexes could be used to create the scale of their thermodynamic/kinetic hydricity by evaluating the impact of the ligand.



Scheme 2. Representation of the Mn–H complexes 1–4 which are the subject of this study.

2. Results and Discussion

2.1. Interaction of Tricarbonyl Manganese Hydrides 1–4 with Bases

Hydrogen bonding. Addition of Lewis bases (**LB**) such as pyridine and hexamethylphosphoramide (HMPA) to complex *mer,trans*-[(P(OPh)₃)₂Mn(CO)₃H] (**1**) in methylcyclohexane (MCH) at 190 K leads to weak hydrogen bond formation where Mn–H serves as a proton donor [22–25]. Hydrogen bonding was evidenced by the appearance of a low-frequency shoulder at the initial ν_{CO} 1958 cm^{−1} band ($\Delta\nu$ 5–20 cm^{−1}) (Figure S1). Since hydrogen bonding is a reversible process, a temperature increase up to 290 K shifts the equilibrium (Scheme 1, path a) towards free manganese hydride. Complex *fac*-[(dppm)Mn(CO)₃H] (**3**) also forms a hydrogen bond with these bases; its three ν_{CO} bands (1996, 1916, 1909 cm^{−1}) shift to lower frequencies by 3–7 cm^{−1} in the presence of 70 equiv. HMPA (Figure S2). However, the strength of these bases is insufficient for proton transfer to occur. The change of the nonpolar MCH to polar acetonitrile also does not promote the proton transfer from **3** to pyridine ($pK_a = 12.53$ in MeCN) or HMPA ($pK_a = 6.1$ in CH₃NO₂).

Proton transfer. Quantitative deprotonation of **1** was observed in acetonitrile when a stronger base—1,8-diazabicyclo[5.4.0]undec-7-ene (DBU; $pK_a = 24.31$ in MeCN)—was used. Full conversion of **1** to anionic complex [(P(OPh)₃)₂Mn(CO)₃][−][HDBU]⁺ (**1**[−]) was confirmed by ³¹P NMR in CD₃CN, since the initial signal at δ_P 183.3 ppm converts into downfield resonance δ_P 206.5 ppm after DBU addition (the key spectral parameters for this and all other complexes studied are summarized in Table 1). To explore the features of proton transfer equilibrium (Scheme 1, path a), we decided to return into a non-polar solvent that should impede proton transfer process. Indeed, in methylcyclohexane the proton transfer is temperature dependent and starts when the reaction mixture is cooled below 260 K. According to IR spectra, the addition of 1.1 equiv. DBU to a solution of **1** in MCH at low temperatures (190–260 K) leads to the appearance of anionic manganese species [(P(OPh)₃)₂Mn(CO)₃][−] (**1**[−], ν_{CO} 1815 cm^{−1}) at the expense of the initial complex (ν_{CO} 1958 cm^{−1}). Unexpectedly, proton transfer is slow at these temperatures, taking 1.2 h at 230 K to reach the equilibrium (Figure S3). The rate constants analysis gave the activation energies (See Supplementary Materials for more details) for the proton transfer step: $\Delta H^\ddagger = 7.5$ kcal/mol, $\Delta S^\ddagger = -26$ cal/(mol·K), $\Delta G^\ddagger_{298\text{K}} = 15.3$ kcal/mol. Since the system does come to equilibrium, the experimental equilibrium constants with thermodynamic parameters of proton transfer in MCH were obtained: $\Delta H^\circ = -13.1$ kcal/mol, $\Delta S^\circ = -50$ cal/(mol·K), $\Delta G^\circ_{298\text{K}} = 1.9$ kcal/mol (See Supplementary Materials for more details). The reaction of **1** with a slightly weaker base [Bu₄N]⁺[4-NO₂C₆H₄O][−] ($pK_a = 20.7$ in MeCN [26]) immediately reaches equilibrium in MeCN with the formation of only ~30% proton transfer product (Figure S4). The known acidity constant of 4-NO₂C₆H₄OH allows an estimation of complex **1** acidity $pK_a(\mathbf{1}) = 21.3$.

Table 1. IR and $^{31}\text{P}\{^1\text{H}\}$ NMR data for neutral, cationic and anionic manganese species 1–4 in different solvents.

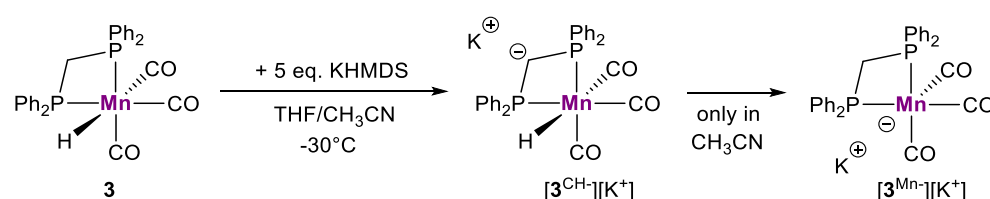
Complex	ν_{CO} (cm^{-1})	δ_{P} (ppm)
1, [(P(OPh) ₃) ₂ Mn(CO) ₃ H]	2040w, 2028w, 1956s ^a	183.3
	2041w, 2028w, 1955s ^b	
	2043w, 2031w, 1958s ^c	
1 ⁺ , [(P(OPh) ₃) ₂ Mn(CO) ₃][HB(C ₆ F ₅) ₃]	2011s, 1969s ^a	153.5
1 ⁻ , [(P(OPh) ₃) ₂ Mn(CO) ₃][HDBU]	1815s ^c	206.5
2, [(PPh ₃) ₂ Mn(CO) ₃ H]	1908s, 1900s ^f	80.5
2 ⁺ , [(PPh ₃) ₂ Mn(CO) ₃] ⁺ [HB(C ₆ F ₅) ₃] ⁻	1980s, 1930s ^f	61.8
2 ⁻ , [(PPh ₃) ₂ Mn(CO) ₃] ⁻ [K ⁺]	1770s, 1741s ^e	-
3, [(dppm)Mn(CO) ₃ H]	1996s, 1916s, 1909s ^a	30.1 ^a
	1993s, 1914s, 1903s ^b	31.8 ^b
<i>fac</i> -3 ⁺ , [(dppm)Mn(CO) ₃][HB(C ₆ F ₅) ₃] [27]	2040s, 1973s, 1935s ^d	10.1
<i>mer</i> -3 ⁺ , [(dppm)Mn(CO) ₃][HB(C ₆ F ₅) ₃] [27]	2060s, 2003s ^d	10.6, 7.1
3 ^{CH-} , <i>fac</i> -[(CH ⁻ -dppm)Mn(CO) ₃ H][K ⁺]	1957s, 1871s, 1876s ^e	10.9 ^a
	1956s, 1870s ^b	
3 ^{Mn-} , [(dppm)Mn ⁻ (CO) ₃][K ⁺]	1867s, 1779s ^b	29.9 ^b
4, <i>fac</i> -[(P-NHC)Mn(CO) ₃ H]	1989s, 1909s, 1889s ^a	95.8
	1988s, 1907s, 1888s ^d	
<i>fac</i> -4 ⁺ , [(P-NHC)Mn(CO) ₃][HB(C ₆ F ₅) ₃]	2032s, 1949s, 1921s ^d	78.1, 71.1 ^f
<i>mer</i> -4 ⁺ , [(P-NHC)Mn(CO) ₃][HB(C ₆ F ₅) ₃]	2038s, 1968s, 1942s ^d	-

^a toluene, ^b MeCN, ^c MCH, ^d *n*BuCl, ^e THF, ^f CH₂Cl₂.

Manganese catalyzed transfer hydrogenation reactions are usually carried out in the presence of strong bases such as potassium *tert*-butylate or KHMDS [1,3,4]. A possible reaction mechanism includes Mn–H bond deprotonation with formation of anionic complex, which participates in further catalytic transformations [3]. We have tried multiple times to identify the conditions for proton abstraction from *mer,trans*-[(PPh₃)₂Mn(CO)₃H] (**2**) and *fac*-[(dppm)Mn(CO)₃H] (**3**), where the Mn–H bond is expected to be rather electron-rich due to the presence of phosphine ligands. However, no repolarization of the Mn–H bond and proton transfer was observed for hydride complexes **2** and **3** with various bases (pyridine, HMPA, DBU, TBD (1,5,7-triazabicyclo[4.4.0]dec-5-ene, $pK_a = 26.03$ in MeCN [28])) even in polar solvents (MeCN, THF). Fortunately, treatment of complex **2** at ambient temperature in THF with KHMDS excess (2 equiv., $pK_a = 26$ in THF [29]) led to partial proton transfer indicated by the appearance of two new low-frequency ν_{CO} bands at 1770 and 1741 cm^{-1} in IR spectrum that correspond to anionic complex **2⁻** (Figure S5) [30]. From these spectral data the pK_a value 27.3 for manganese hydride **2** in THF was estimated.

The reaction of hydride complex **3** with KHMDS (5 equiv.) in THF leads to full proton transfer and the appearance of three new low-frequency-shifted CO bands (1957, 1871, 1876 cm^{-1}) in the IR spectra (Figure 1). The shift of ν_{CO} bands by ca. 40 cm^{-1} in the IR spectra is not consistent with the presence of the negative charge at the metal atom in the case of Mn–H bond deprotonation. Moreover, ^1H NMR spectrum shows the presence of a triplet signal at $\delta_{\text{H}} -5.54$ ppm in the hydride region, while for the initial complex **3** the hydride signal ($\delta_{\text{H}} -5.53$ ppm) is a triplet of doublets due to the $^2J_{\text{PH}}$ and an additional $^4J_{\text{HH}}$ spin-spin interaction with one of the CH₂ bridge H-atoms. The phosphorus resonance observed in this **3**/KHMDS mixture by $^{31}\text{P}\{^1\text{H}\}$ NMR spectroscopy is shifted to stronger field (δ_{P} 10.9) relative to that (δ_{P} 30.1) of the initial manganese hydride **3** (Figure S6). These spectral data allow the proposal that deprotonation occurs at the bridging CH₂ group of dppm ligand with the formation of [**3^{CH-}**][K⁺]. In the ^{13}C spectrum, the triplet (δ_{C} 20.8, $t, ^1J_{\text{CP}} = 51.4$ Hz, PCHP) of corresponding anionic carbon CH⁻ is also shifted to stronger field compared to

the CH₂ signal of **3** (δ_C 48.0, t, $^1J_{CP}$ = 22.4 Hz, PCH₂P). The estimated pK_a value of methylene CH-proton in complex **3** equals 26 in THF. A more polar acetonitrile deprotonation of **3** by the same amount of KHMDS goes through [3^{CH-}][K⁺] formation yielding ultimately the anionic manganese complex [3^{Mn-}][K⁺] (Scheme 3). In the IR and NMR spectra, measured immediately after mixing, three manganese species could be observed; however, in 15 min, the intermediate [3^{CH-}][K⁺] (ν_{CO} 1956, 1870 cm⁻¹; δ_P 10.4 ppm) completely transforms into the final species [3^{Mn-}][K⁺] (ν_{CO} 1867, 1779 cm⁻¹; δ_P 29.9 ppm) (Figures 1 and S6) that has no hydride signal in the ¹H NMR spectrum. According to our DFT calculations, the intramolecular proton transfer from manganese to the anionic bridge CH is explained by thermodynamic preference of the metal deprotonated form (ΔG_{298K} = -0.2 kcal/mol) in acetonitrile compared with THF (Table 2). That implies that even manganese complexes with pronounced hydride character [11,17] can be deprotonated by KHMDS, thus allowing the corresponding anionic intermediates to participate in hydrogenation reactions.



Scheme 3. Formation of [3^{Mn-}][K⁺] from **3** by addition of KHMDS.

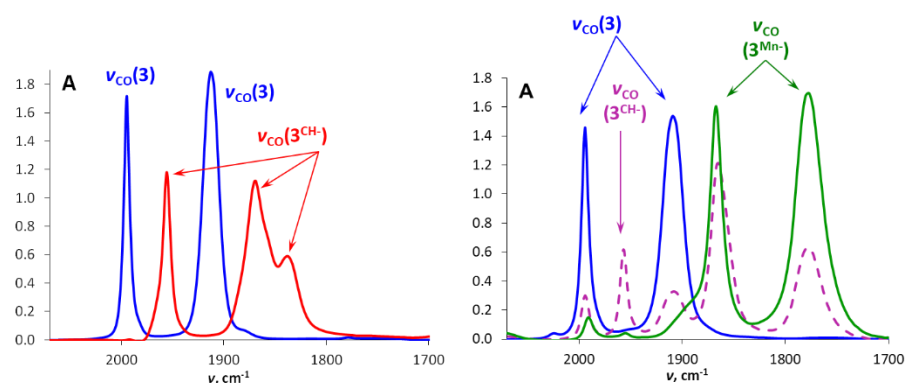


Figure 1. IR spectra of *fac*-[(dppm)Mn(CO)₃H] (**3**) (*c* = 0.01 M) alone (blue) and after KHMDS addition (5 equiv.; red/green). (Left)—THF, (right)—MeCN (*l* = 0.01 cm, 295 K).

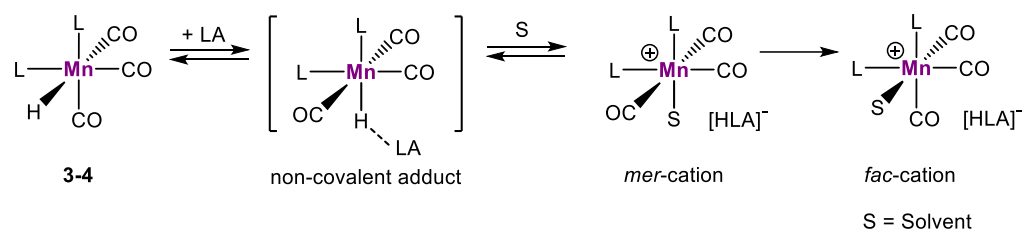
Table 2. Relative energies (in kcal/mol) of the complex [3^{Mn-}][K⁺] formation computed at DFT/ ω B97XD/def2-TZVP level. Complex [3^{Mn-}][K⁺] is taken as a zero.

	Toluene	THF	MeCN
E _{el}	+2.8	-0.7	-3.1
ΔH	+5.7	+2.0	-0.2
ΔG	+7.6	+2.5	-0.2

2.2. Interaction of Tricarbonyl Manganese Hydrides with Lewis Acids

Non-covalent adducts. Interaction of manganese hydride complexes (**1–4**) with Lewis acids (LA) leads to Mn–H bond polarization, making the hydride atom more negatively charged. Recently, we have proven that the formation of non-covalent adducts between Lewis acid and hydride complex *fac*-[(dppm)Mn(CO)₃H] (**3**) at 180 K precedes the hydride ion abstraction [27] (Scheme 4). Noteworthy, while the initial hydride **3** has *facial* geometry, the most stable form of the non-covalent adduct is the isomer with the *meridional* geometry. The latter then undergoes additional transformations, including intramolecular hydride transfer with the formation of *meridional* cation stabilized by the solvent molecule

mer-[(dppm)Mn(CO)₃(κ¹Cl-CH₂Cl₂)](HBAr₃) and its isomerization to a more stable *facial* isomer *fac*-[(dppm)Mn(CO)₃(κ¹Cl-CH₂Cl₂)](HBAr₃).



Scheme 4. Isomerization process of complexes 3–4 into more stable *facial* isomers.

The analogous chemical behavior was observed upon addition of B(C₆F₅)₃ to complex *fac*-[(P-NHC)Mn(CO)₃H] (**4**) at 180 K in methylene chloride. The Lewis acid coordination to the hydride ligand and formation of the non-covalent adduct **4**⋯LA gives in ¹H NMR spectrum a broadened resonance at δ_H −7.98 ppm shifted high-field relative to the initial signal of **4** (δ_H −7.42) (Figure 2). A weak Brønsted acid *mer,trans*-[(P(OPh)₃)₂Mn(CO)₃H] (**1**) also interacts with Lewis acids as a hydride-ion donor. Addition of B(C₆F₅)₃ (10 equiv.) to the toluene solution of **1** (ν_{CO} 2040w, 2028w, 1956s cm^{−1}) at 190 K leads to the formation of a non-covalent complex **1**⋯B(C₆F₅)₃ (ν_{CO} 2035s, 1973s cm^{−1}). We assume that this adduct has a *facial* configuration, since its ν_{CO} bands are strongly shifted to high frequencies (*cf.* 2046s, 1980s cm^{−1} for *fac*-**1** and 2026w, 1942s cm^{−1} for *mer,trans*-**1** in *nujol*) [31]. Formation of non-covalent adduct with B(C₆F₅)₃ stabilizes *fac*-**1** and in the 190–220 K temperature range the equilibrium between two species, *mer,trans*-**1** and *fac*-**1**⋯B(C₆F₅)₃, is observed in the IR spectra (Figure S7). In ¹H NMR spectra of the **1** + B(C₆F₅)₃ mixture, measured under the same conditions, the formation of the intermediate complex *fac*-**1**⋯B(C₆F₅)₃ is evidenced by new broad hydride resonance shifted to the higher field (δ_H −9.36 ppm) (Figure S8, *left*). In ³¹P{¹H} NMR spectra (Figure S8, *right*), the resonance at δ_P 163 ppm exhibits the same temperature behavior and can be attributed to *fac*-**1**⋯B(C₆F₅)₃. Thus, complex **1** is the least reactive toward hydride transfer (see below) and its non-covalent adduct with Lewis acid exists in a wider temperature range.

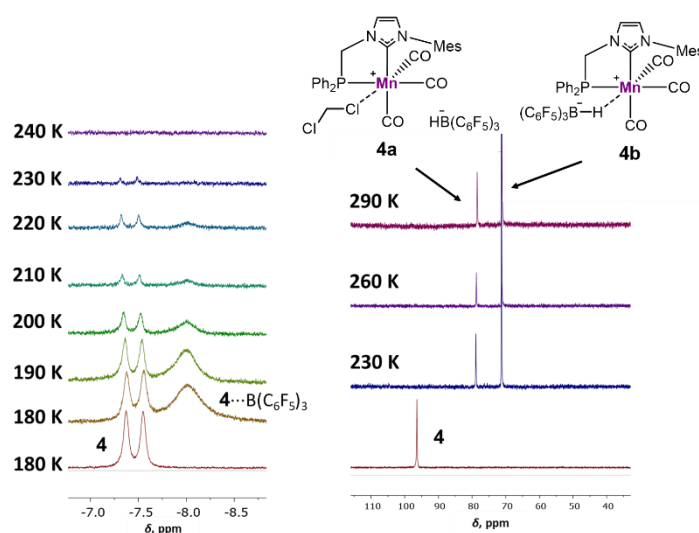


Figure 2. Variable temperature ¹H (300 MHz) and ³¹P{¹H} (162.0 MHz) NMR spectra of complex **4** in CD₂Cl₂ solution (bottom lines) and its mixture with B(C₆F₅)₃.

Hydride transfer. The non-covalent adducts **1**⋯LA–**4**⋯LA precede the intramolecular hydride transfer that yields the cationic complexes with different geometries, which are stabilized by coordination of solvent molecule or [H-LA][−] anion. Thus, for *fac*-[(P-

NHC)Mn(CO)₃H] (**4**) interacting with B(C₆F₅)₃ at 180 K, new high-frequency ν_{CO} bands at 2038, 1968 and 1942 cm⁻¹ appear in the IR spectrum assigned to the cationic *mer*-intermediate; at 190 K they already transform into *fac*-product with ν_{CO} bands at 2032, 1949 and 1921 cm⁻¹ (Figure S9). In contrast to isostructural *fac*-[(dppm)Mn(CO)₃H] (**3**), in the case of complex **4** two configurations are possible when Mn(CO)₃ moiety is in meridional arrangement: hydride ligand being *trans* to the phosphorus atom (*mer*-P-**4**) or *trans* to the NHC carbon atom (*mer*-C-**4**) (Figure S8). Since complex *mer*-P-**4** should feature more hydridic H-atom than *mer*-C-**4** due to the higher *trans*-effect of phosphorus [32], we assumed that the hydride transfer occurs through the formation of the meridional *trans*-to-P form (*mer*-P-**4**⋯B(C₆F₅)₃).

Above 230 K, the equilibrium is completely shifted to cationic products, the ³¹P{¹H} spectrum contains only two resonances δ_P 78.0 and 71.0 ppm in 1:4 ratio (Figure 2). After 4 days at room temperature, this ratio inverts and becomes 2:1. By selectively decoupling ³¹P, the CH₂-bridge H-atoms δ_H 5.07 (dd, ²J_{HH} = 14.0, ²J_{PH} = 5.1 Hz) and 4.94 (dd, ²J_{HH} = 14.1, ²J_{PH} = 6.6 Hz) can be attributed to complex **4a** with δ_P 78.1 ppm and δ_H 5.48 (vt, ²J_{HH} = 14.4 Hz, ²J_{PH} = 13.7 Hz) and 4.99 (d, ²J_{HH} = 14.4 Hz) to complex **4b** δ_P 71.1. While the ³¹P{¹H} resonance of **4a** shifts (74.1–78.1 ppm) in response to changing the solvent (toluene, *n*BuCl, C₆H₅Cl, CD₂Cl₂), the chemical shift of **4b** keeps its position (Table S1). Thus, we suggest that the two cationic products are [(P-NHC)Mn(CO)₃(Solvent)]⁺[HB(C₆F₅)₃]⁻ (**4a**), which has a coordinated solvent molecule, and [(P-NHC)Mn(CO)₃]⁺[HB(C₆F₅)₃]⁻ (**4b**), which is a contact ionic pair stabilized by B–H bond interaction with the cationic metal center (**4b**) remains in tranquility. The sensitivity of the ³¹P{¹H} resonance of **4a** to the media is indicative of the solvent's influence on its structure. To obtain an independent proof of its structure, we reacted the manganese bromide *fac*-[(P-NHC)Mn(CO)₃Br] with AgBF₄ in MeCN as a solvent. The cationic complex **4**^{MeCN} obtained features acetonitrile molecule coordinated to the metal center as it was confirmed by X-ray diffraction (Figure 3), and its ³¹P{¹H} resonance (77.5 ppm in CD₂Cl₂) is in the range of **4a**-type complexes.

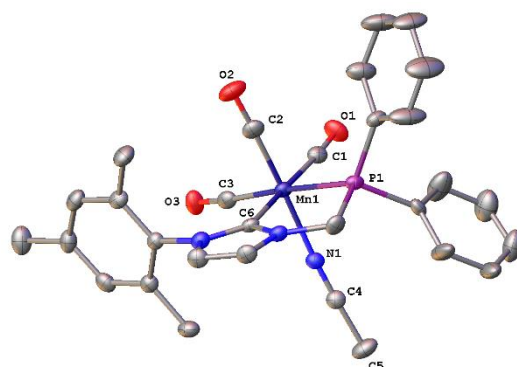
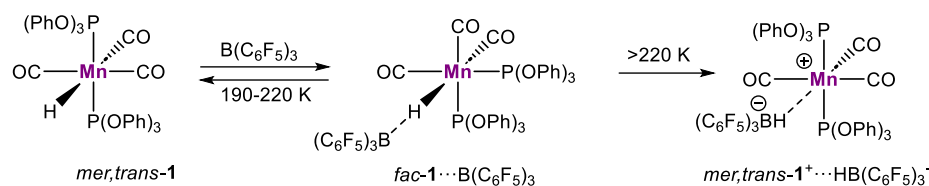


Figure 3. Molecular structure of the cationic complex *fac*-[(P-NHC)Mn(CO)₃(MeCN)]⁺[BF₄]⁻ (**4**^{MeCN}) (40% probability ellipsoids, only one crystallographically independent molecule in the cell is shown). Counter-anions and hydrogen atoms are omitted for clarity. Selected bond lengths (Å): Mn1–N1 2.011(4), Mn1–P1 2.317(1), Mn1–C6 2.048(5), C1–O1 1.146(7), C2–O2 1.156(6), C3–O3 1.146(5), Mn1–C1 1.817(6), Mn1–C2 1.786(5), Mn1–C3 1.835(4), N1–C4 1.130(6).

For the non-covalent complex *fac*-**1**⋯B(C₆F₅)₃ the hydride transfer occurs above 230 K (Scheme 5). The single product of the hydride transfer is a cationic manganese complex *mer,trans*-[**1**]⁺[HB(C₆F₅)₃]⁻. The signal of the cationic product [1]⁺[HB(C₆F₅)₃]⁻ becomes clearly seen in ³¹P spectra at 250 K (δ_P 153.0 ppm).



Scheme 5. Formation of complex *mer,trans*-[1]⁺[HB(C₆F₅)₃]⁻ from **1** in the presence of B(C₆F₅)₃.

Structurally similar complex *mer,trans*-[(PPh₃)₂Mn(CO)₃H] (**2**) bearing more donating phosphine ligands was found to be more reactive. Indeed, it transforms into *mer,trans*-[(PPh₃)₂Mn(CO)₃(solv)][HB(C₆F₅)₃] (**2**⁺) already at 180 K (Figure S11). IR spectra in the 180–250 K range show the transformation of hydride **2** directly into cationic complex [**2**⁺][HB(C₆F₅)₃]⁻ (ν_{CO} 1980, 1930 cm⁻¹) without detectable non-covalent adduct formation and *mer*-to-*fac* isomerization. At temperatures higher than 250 K, partial decomposition of this cationic species was observed, resulting in the formation of known tetracarbonyl complex *trans*-[(PPh₃)₂Mn(CO)₄]⁺ exhibiting a ν_{CO} band at 2002 cm⁻¹ [33]. ³¹P{¹H} NMR spectra confirm the formation of sole cationic product (δ_P 61.8 ppm) and its further decomposition. Direct synthesis of *mer,trans*-[(PPh₃)₂Mn(CO)₃(CH₃CN)]⁺[BF₄]⁻ **2**^{MeCN} allows the formation of a stable cationic product with ν_{CO} at 2055w, 1977s, 1946s cm⁻¹ characterized by X-ray diffraction (Figure 4).

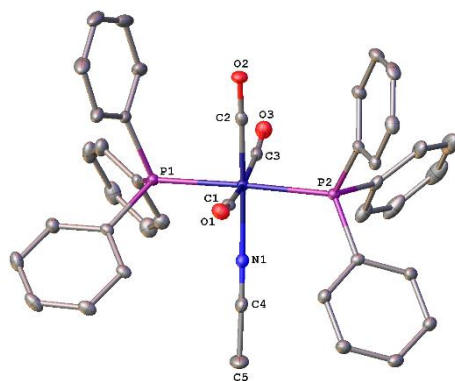


Figure 4. Molecular structure of the cationic complex *mer,trans*-[(PPh₃)₂Mn(CO)₃(CH₃CN)]⁺ **2**^{MeCN} (40% probability ellipsoids, tetrafluoroborate anion, solvate molecule of dichloromethane and hydrogen atoms are omitted for clarity). Selected bond lengths (Å): Mn1–N1 1.999(3), Mn1–P1 2.3337(8), Mn1–P2 2.3329(8), C1–O1 1.140(3), C2–O2 1.149(4), C3–O3 1.137(3), Mn1–C1 1.857(3), Mn1–C2 1.794(3), Mn1–C3 1.860(4), N1–C4 1.134(4).

2.3. Kinetic Hydricity of Manganese Tricarbonyl Complexes

The hydride transfer from complexes **1–4** to B(C₆F₅)₃ is relatively slow at low temperatures that allow the estimation of their kinetic hydricities (See Supplementary Materials for more details; Figures S12 and S13). The low-temperature IR monitoring of hydride transfer kinetics in the presence of 1.1 equiv. B(C₆F₅)₃ in *n*BuCl gave effective rate constants (*k*_{eff}). The value of free energy Δ*G*[‡]_{298K} characterizes the kinetic hydricity of manganese complexes but depends on the Lewis acidity of the given hydride abstractor. As expected, the hydride complex **1**, which is a weak acid due to electron-withdrawing phosphite ligands, has the lowest hydricity (Δ*G*[‡]_{298K} = 19.8 kcal/mol), while complex **4** bearing phosphine-carbene ligand, the most electron-rich in this series, possesses the highest Δ*G*[‡]_{298K} = 16.5 kcal/mol among the complexes studied (Table 3). The kinetic hydricity of the manganese complexes of interest increases in the order *mer,trans*-[(P(OPh)₃)₂Mn(CO)₃H] (**1**) < *mer,trans*-[(PPh₃)₂Mn(CO)₃H] (**2**) ≈ *fac*-[(dppm)Mn(CO)₃H] (**3**) < *fac*-[(P-NHC)Mn(CO)₃H] (**4**), reflecting the gain of the phosphorus ligand electron donor properties (basicity). On the activation free energy scale (Δ*G*[‡]_{298K}) there is only small by 0.5 kcal/mol difference be-

tween complexes 2–4 bearing electron-donating ligands. However, the distinction between their properties becomes more pronounced at lower temperatures due to the impact of highly negative activation entropy ΔS^\ddagger (cf. $k_{\text{eff } 220\text{K}}$, Table 3).

Table 3. Effective rate constants for the interaction between 1–4 and $\text{B}(\text{C}_6\text{F}_5)_3$ in $n\text{BuCl}$ at 220 K and activation parameters of hydride transfer.

MnH	$k_{\text{eff } 220\text{K}}$, $\text{M}^{-1}\cdot\text{s}^{-1}$	ΔH^\ddagger , kcal/mol	ΔS^\ddagger , cal/(mol·K)	$\Delta G^\ddagger_{220\text{K}}$, kcal/mol	$\Delta G^\ddagger_{298\text{K}}$, kcal/mol
1	0.00008	8.6 ± 0.2	-37 ± 1	16.9 ± 0.1	19.8 ± 0.1
2	0.147	4.1 ± 0.5	-43 ± 3	13.6 ± 0.3	17.0 ± 0.3
3	0.006	9.4 ± 0.6	-26 ± 3	15.0 ± 0.2	17.0 ± 0.2
4	0.706	3.8 ± 0.2	-43 ± 1	13.2 ± 0.1	16.5 ± 0.1

3. Materials and Methods

All reactions were performed using standard Schlenk procedures under a dry argon atmosphere. Dry and oxygen-free organic solvents (toluene, THF) were obtained using a solvent purification system from M. Braun (Germany). Methylcyclohexane was dried over Na and distilled under an argon atmosphere. $n\text{BuCl}$, CH_2Cl_2 and acetonitrile were stored over CaH_2 and distilled under an argon atmosphere before use. Deuterated solvents for NMR were degassed before use by three freeze–pump–thaw cycles and kept over 3\AA molecular sieves. A liquid nitrogen/ethanol or nitrogen/isopropanol slush bath was used to maintain samples at the desired low temperature.

Variable-temperature (VT) NMR spectra were recorded on Bruker Avance 300, Bruker Avance 400 (Bruker, Billerica, MA, USA) and Varian Inova 400 (Varian, USA) spectrometers operating at 300 and 400 MHz in the 180–300 K temperature range. ^1H and $^{13}\text{C}\{^1\text{H}\}$, chemical shifts are reported in parts per million (ppm) downfield of tetramethylsilane (TMS) and were calibrated against the residual resonance of the deuterated solvent, while $^{31}\text{P}\{^1\text{H}\}$ chemical shifts were referenced to 85% H_3PO_4 with downfield shift taken as positive. The IR spectra were recorded at different temperatures (160–293 K) using a home-modified cryostat (Carl Zeiss Jena) with a Nicolet iS50 FTIR (Thermo Scientific, USA) spectrometer using 0.05 cm CaF_2 cells. The accuracy of the experimental temperature adjustment was ± 0.5 °C. The cryostat modification allowed the transfer of the reagents (premixed at either low or room temperature) under an inert atmosphere directly into the cells.

Manganese hydride complexes *mer,trans*- $[(\text{P}(\text{O}Ph)_3)_2\text{Mn}(\text{CO})_3\text{H}]$ (1) [31], *mer,trans*- $[(\text{PPh}_3)_2\text{Mn}(\text{CO})_3\text{H}]$ (2) [34], *fac*- $[(\text{dppm})\text{Mn}(\text{CO})_3\text{H}]$ (3) [27] and *fac*- $[(\text{P-NHC})\text{Mn}(\text{CO})_3\text{H}]$ (4) [4] (Scheme 2) were prepared according to the literature methods. Commercially available tris(pentafluorophenyl)boron was purified by sublimation before use. All other reagent-grade chemicals purchased from commercial sources were used as received.

Synthesis of *fac*- $[(\text{P-NHC})\text{Mn}(\text{CO})_3(\text{MeCN})]\text{BF}_4$ (4^{MeCN}).

AgBF_4 (0.375 mmol, 73 mg) was placed into the Schlenk flask containing *fac*- $(\text{P-NHC})\text{Mn}(\text{CO})_3\text{Br}$ (0.375 mmol, 226 mg) under inert atmosphere. Then 5 mL of CH_3CN was added upon stirring at room temperature. The obtained suspension was sonicated for 5 min and left stirring overnight till complete product formation that was controlled by the IR spectroscopy. After that, the CH_3CN was removed under reduced pressure, the yellow oil residue was dissolved in 5 mL of CH_3CN again to avoid colloid solution formation. The resulting solution was separated from the precipitate via filtration through a Pasteur pipette with Celite, concentrated to 1/10 of initial volume, and dry Et_2O (80 mL) was added dropwise to induce precipitation of the product. The precipitate was left under supernatant overnight at -20 °C. The next day, the supernatant was removed, and the precipitate was washed with 5 mL two times and dried in a vacuum yielding (211 mg, 86%) pale-yellow powder.

Synthesis of *mer,trans*- $[(\text{PPh}_3)_2\text{Mn}(\text{CO})_3(\text{CH}_3\text{CN})]\text{BF}_4$ (2^{MeCN}).

A suspension of $(PPh_3)_2Mn(CO)_3H$ (0.008 mmol, 5.0 mg) and $[Ph_3C][BF_4]$ (0.008 mmol, 2.6 mg) in CH_3CN (5 mL) was placed in the ultrasonic bath for 5 min at room temperature and left stirring till complete product formation that was controlled by the IR spectroscopy. The solvent was removed under reduced pressure. The resulting pale-yellow solid was dissolved in CH_2Cl_2 (1 mL) and then filtered through a Pasteur pipette with Celite. Hexane (5 mL) was added to the solution to induce crystallization. The supernatant was removed by decantation, the crystalline precipitate was washed with hexane (2×5 mL) and then dried in the vacuum to yield $[(PPh_3)_2Mn(CO)_3(CH_3CN)][BF_4]$ (4.6 mg, 76%) as pale-yellow crystals.

Structures of reactants and complexes were optimized at the ω B97-XD level [35], applying def2-TZVP basis set [36] by Gaussian 09 [37]. Optimizations were done in toluene, THF and CH_3CN introduced by a SMD solvent model [38].

Cationic complexes *mer,trans*- $[(PPh_3)_2Mn(CO)_3(MeCN)][BF_4]$ 2^{MeCN} and *fac*- $[(P-NHC)Mn(CO)_3(MeCN)][BF_4]$ 4^{MeCN} were crystallized from the CH_2Cl_2 /hexane system. X-ray diffraction data were collected at 100 K with a Bruker Quest D8 CMOS diffractometer (Bruker, MA, USA), using graphite monochromated Mo-K α radiation ($\lambda = 0.71073 \text{ \AA}$). Using Olex2 [39], the structures were solved with the ShelXT [40] structure solution program using Intrinsic Phasing and refined with the XL [41] refinement package using Least-Squares minimization against F^2 in anisotropic approximation for non-hydrogen atoms. Positions of hydrogen atoms were calculated, and they were refined in the isotropic approximation within the riding model. Crystal data and structure refinement parameters are given in Table S2. CCDC 2241621 and 2241622 contain the supplementary crystallographic data for 2^{MeCN} and 4^{MeCN} , respectively.

3.1. General Procedure for the Interaction with Bases

For variable temperature IR studies.

The solution of *mer,trans*- $[(P(OPh)_3)_2Mn(CO)_3H]$ (**1**, $c = 0.003$ M) was prepared at room temperature in methylcyclohexane. Then it was placed into a cryostat and cooled to 190 K. After the spectrum of the initial complex was acquired, the solution from the cryostat was added to the solution of corresponding base (pyridine, HMPA, DBU; 1–70 eq., $c = 0.003$ – 0.21 M dissolved in a small amount of solvent kept at 190 K in liquid nitrogen/*i*PrOH slush bath). The mixture obtained was quickly returned into the cryostat, and the IR spectra were monitored in the 190–290 K temperature range.

Solid *fac*- $[(dppm)Mn(CO)_3H]$ (**3**, $m = 10.0$ mg, $n = 0.02$ mmol) and KHMDS ($m = 11.5$ mg, $n = 0.10$ mmol) were placed in separate Schlenk tubes under inert atmosphere. The complex was dissolved in THF or acetonitrile at room temperature, and a small aliquot was taken to IR cell. After the spectrum of the initial complex was acquired, the Schlenk tubes with solution and solid KHMDS were cooled to 243 K in a liquid nitrogen/ethanol slush bath. Then the solution of complex **3** was quickly transferred to KHMDS with a Pasteur pipette, and the obtained mixture was stirred and transferred into the IR cell at room temperature for spectrum acquisition.

For variable temperature NMR studies.

Solid *fac*- $[(dppm)Mn(CO)_3H]$ (**3**, $m = 20$ mg, $n = 0.04$ mmol) and KHMDS ($m = 23$ mg, $n = 0.20$ mmol) were placed in separate Schlenk tubes under inert atmosphere. The complex was dissolved in THF-*d*₈ or CD_3CN at room temperature. After that, the NMR tube under inert atmosphere and Schlenk tubes with solution and solid KHMDS were cooled to 243 K in a liquid nitrogen/ethanol slush bath. The solution of complex **3** was transferred to KHMDS with a Pasteur pipette, and the obtained mixture was stirred and quickly filtered through glass cotton directly into precooled NMR tube. The resulting NMR sample was inserted into a pre-cooled NMR probe at 243 K and then monitored with multi-nuclear NMR spectroscopy at 243 K.

3.2. General Procedure for the Interaction with Lewis Acid

For variable temperature NMR studies.

The chosen amount of *mer,trans*-[(P(OPh)₃)₂Mn(CO)₃H] (**1**, *m* = 5.3 mg, *n* = 0.007 mmol) was dissolved in toluene-*d*₈ at room temperature and monitored in the 200–293 K temperature range. Then the solution of B(C₆F₅)₃ (7 eq., *m* = 25 mg, *n* = 0.007 mmol in 0.5 mL toluene-*d*₈) was added at 200 K, and the reaction mixture was monitored at 200–293 K.

Similarly, complexes **2–4**, (*m* = 20 mg, *n* = 0.04 mmol) were dissolved in CD₂Cl₂, placed into an NMR tube and frozen in liquid nitrogen. Then the solution of the Lewis acid (B(C₆F₅)₃; 1 eq., *n* = 0.04 mmol) in CD₂Cl₂ was poured over the frozen solution in the NMR tube. Two frozen solutions were simultaneously melted in a slush nitrogen/EtOH bath at 180 K, and then the mixture obtained was monitored in the 183–293 K temperature range.

For variable temperature IR studies.

The solution of *mer,trans*-[(P(OPh)₃)₂Mn(CO)₃H] (**1**, *c* = 0.005 M) was prepared at room temperature in toluene. Then it was placed into a cryostat and cooled to 190 K. After the spectrum of the initial complex was acquired, the solution from the cryostat was added to B(C₆F₅)₃ (10 eq., *c* = 0.05 M) and dissolved in a small amount of solvent kept at 190 K in a nitrogen/*i*PrOH slush bath. The obtained mixture was quickly returned to the cryostat and monitored in the 190–290 K temperature range.

The solutions of complexes **2–4** (*c* = 0.003 M) were prepared at room temperature in *n*BuCl (CH₂Cl₂ or toluene). Then, they were placed into a cryostat and cooled to 160 K (180 K or 190 K). After the spectrum of the initial complex was acquired, the solution from the cryostat was added to the corresponding Lewis acid B(C₆F₅)₃ (1–1.3 eq., *c* = 0.003–0.004 M), dissolved in a small amount of solvent and cooled to 160 K (180 K or 190 K) in a nitrogen/EtOH (nitrogen/*i*PrOH) slush bath. The obtained mixture was quickly returned to the cryostat and monitored in the 160 (180 or 190)–290 K temperature range.

4. Conclusions

In conclusion, we have shown that tricarbonyl manganese hydride complexes exhibit *dual* reactivity under *Lewis* acid or base treatment. Even the complexes with pronounced hydride character (**2**, **3**) can be deprotonated or, *vice versa*, the complex with acidic properties (**1**) can serve as a hydride donor. The Mn–H bond repolarization occurs at the stage of formation of non-covalent intermediates with *Lewis* acid or base as exemplified for complex **1**. The strength of these non-covalent bonds determines whether subsequent hydrogen ion (hydride or proton) transfer will occur. The studies on the complexes bearing bidentate ligands, *fac*-[(L-L')Mn(CO)₃H] (**3**, **4**), revealed that their reactions do not follow simple mechanisms but rather involve the *fac*-to-*mer* isomerizations. The hydride abstraction from these hydrides proceeds from the *mer*-derivatives in which the hydride ligand located *trans* to electron-donating phosphine ligand is more reactive relative to *fac*-isomers where hydride is *trans* to CO ligand. Interestingly, the initial deprotonation site of complex **3** in acetonitrile was observed at the CH₂ bridge of the dppm ligand, providing the expected metal-deprotonated product via proton migration from anionic hydride intermediate. Since anionic or cationic Mn(I) complexes formed as the result of proton or hydride abstraction are potential intermediates of (de)hydrogenation reactions, quantitative values of kinetic hydricity of the hydride complexes obtained herein may correlate with their potential catalytic activity and be useful for further elucidation of reaction mechanisms.

Supplementary Materials: The following supporting information can be downloaded at: www.mdpi.com/xxx/s1: IR and NMR spectroscopic characterization of Mn(I) hydride, cationic and anionic complexes; crystal data and structure refinement parameters; details of thermodynamic and kinetic parameters determination.

Author Contributions: Investigation, E.S.O., S.A.K., E.S.G., N.V.K., A.A.P., O.A.F., D.A.V. and A.A.D.; Writing—Original Draft Preparation, E.S.O.; Writing—Review and Editing, N.V.B., D.A.V. and Y.C.; Supervision, E.S.S. and N.V.B. All authors have read and agreed to the published version of the manuscript.

Funding: This work was financially supported by the Russian Science Foundation (grant No. 22-73-00072).

Institutional Review Board Statement:

Informed Consent Statement:

Data Availability Statement:

Acknowledgments: D.A.V. and Y.C. thank CNRS for the support. E.S.G. is grateful to the French Embassy in Moscow for a joint PhD fellowship (Vernadski program). Computational studies were performed using HPC resources from CALMIP (grant no. P18038). The NMR and X-ray diffraction data were collected using the equipment of the Center for Molecular Composition Studies of INEOS RAS with the support from the Ministry of Science and Higher Education of the Russian Federation (Contract No. 075-03-2023-642).

Conflicts of Interest: The authors declare no conflict of interest.

References

1. Valyaev, D.A.; Lavigne, G.; Lugan, N. Manganese organometallic compounds in homogeneous catalysis: Past, present, and prospects. *Coord. Chem. Rev.* **2016**, *308*, 191–235.
2. Mukherjee, A.; Milstein, D. Homogeneous catalysis by cobalt and manganese pincer complexes. *ACS Catal.* **2018**, *8*, 11435–11469.
3. Gulyaeva, E.S.; Osipova, E.S.; Buhaibeh, R.; Canac, Y.; Sortais, J.-B.; Valyaev, D.A. Towards ligand simplification in manganese-catalyzed hydrogenation and hydrosilylation processes. *Coord. Chem. Rev.* **2022**, *458*, 214421.
4. Buhaibeh, R.; Filippov, O.A.; Bruneau-Voisine, A.; Willot, J.; Duhayon, C.; Valyaev, D.A.; Lugan, N.; Canac, Y.; Sortais, J.B. Phosphine-NHC manganese hydrogenation catalyst exhibiting a non-classical metal-ligand cooperative H₂ activation mode. *Angew. Chem. Int. Ed.* **2019**, *131*, 6799–6803.
5. Kireev, N.V.; Filippov, O.A.; Gulyaeva, E.S.; Shubina, E.S.; Vendier, L.; Canac, Y.; Sortais, J.-B.; Lugan, N.; Valyaev, D.A. Bis[diphenylphosphino]methane and its bridge-substituted analogues as chemically non-innocent ligands for H₂ activation. *Chem. Commun.* **2020**, *56*, 2139–2142.
6. Pearson, R.G. The transition-metal-hydrogen bond. *Chem. Rev.* **1985**, *85*, 41–49.
7. Crabtree, R.H. *The Organometallic Chemistry of the Transition Metals*; John Wiley & Sons: Hoboken, NJ, USA, 2009.
8. Kristjánssdóttir, S.; Norton, J. *Transition Metal Hydrides*; Dedieu, A., Ed.; 1992; Volume 309.
9. Bullock, R.M. Catalytic ionic hydrogenations. *Chem. Eur. J.* **2004**, *10*, 2366–2374.
10. Jordan, R.F.; Norton, J.R. Kinetic and thermodynamic acidity of hydrido transition-metal complexes. 1. Periodic trends in Group VI complexes and substituent effects in osmium complexes. *J. Am. Chem. Soc.* **1982**, *104*, 1255–1263.
11. Cheng, T.-Y.; Brunschwig, B.S.; Bullock, R.M. Hydride transfer reactions of transition metal hydrides: Kinetic hydricity of metal carbonyl hydrides. *J. Am. Chem. Soc.* **1998**, *120*, 13121–13137.
12. Bullock, R.M. Proton transfer from metal hydrides to metal alkynyl complexes. Remarkable carbon basicity of (C₅H₅)(PMe₃)₂Ru-CC-CMe₃. *J. Am. Chem. Soc.* **1987**, *109*, 8087–8089.
13. Filippov, O.; Golub, I.; Osipova, E.; Kirikina, V.; Gutsul, E.; Belkova, N. Activation of M–H bond upon the complexation of transition metal hydrides with acids and bases. *Russ. Chem. Bull.* **2014**, *63*, 2428–2433.
14. Belkova, N.V.; Filippov, O.A.; Osipova, E.S.; Safronov, S.V.; Epstein, L.M.; Shubina, E.S. Influence of phosphine (pincer) ligands on the transition metal hydrides reactivity. *Coord. Chem. Rev.* **2021**, *438*, 213799.
15. Wiedner, E.S.; Chambers, M.B.; Pitman, C.L.; Bullock, R.M.; Miller, A.J.; Appel, A.M. Thermodynamic hydricity of transition metal hydrides. *Chem. Rev.* **2016**, *116*, 8655–8692.
16. Edidin, R.T.; Sullivan, J.M.; Norton, J.R. Kinetic and thermodynamic acidity of hydrido transition-metal complexes. 4. Kinetic acidities toward aniline and their use in identifying proton-transfer mechanisms. *J. Am. Chem. Soc.* **1987**, *109*, 3945–3953.
17. Sandhya, K.; Suresh, C.H. Quantification of thermodynamic hydricity of hydride complexes of Mn, Re, Mo, and W using the molecular electrostatic potential. *J. Phys. Chem.* **2017**, *121*, 2814–2819.
18. Kuchynka, D.; Amatore, C.; Kochi, J. Electrooxidation of metal carbonyl anions. Formation and reactivity of 17-electron manganese (0) radicals. *J. Organomet. Chem.* **1987**, *328*, 133–154.
19. Belkova, N.V.; Epstein, L.M.; Filippov, O.A.; Shubina, E.S. Hydrogen and dihydrogen bonds in the reactions of metal hydrides. *Chem. Rev.* **2016**, *116*, 8545–8587.
20. Belkova, N.V.; Epstein, L.M.; Shubina, E.S. Dihydrogen bonding, proton transfer and beyond: What we can learn from kinetics and thermodynamics. *Eur. J. Inorg. Chem.* **2010**, *23*, 3555–3565.

21. Ault, B.S.; Becker, T.M.; Li, G.Q.; Orchin, M. The infrared spectra and theoretical calculations of frequencies of fac-tricarbonyl octahedral complexes of manganese (I). *Spectrochim. Acta A Mol. Biomol. Spectrosc.* **2004**, *60*, 2567–2572.
22. Belkova, N.V.; Gutsul, E.I.; Filippov, O.A.; Levina, V.A.; Valyaev, D.A.; Epstein, L.M.; Lledos, A.; Shubina, E.S. Intermolecular hydrogen bonding between neutral transition metal hydrides ($\eta^5\text{-C}_5\text{H}_5$)M(CO)₃H (M = Mo, W) and bases. *J. Am. Chem. Soc.* **2006**, *128*, 3486–3487.
23. Levina, V.A.; Filippov, O.A.; Gutsul, E.I.; Belkova, N.V.; Epstein, L.M.; Lledos, A.; Shubina, E.S. Neutral transition metal hydrides as acids in hydrogen bonding and proton transfer: Media polarity and specific solvation effects. *J. Am. Chem. Soc.* **2010**, *132*, 11234–11246.
24. Levina, V.A.; Rossin, A.; Belkova, N.V.; Chierotti, M.R.; Epstein, L.M.; Filippov, O.A.; Gobetto, R.; Gonsalvi, L.; Lledós, A.; Shubina, E.S. Acid–base interaction between transition-metal hydrides: Dihydrogen bonding and dihydrogen evolution. *Angew. Chem. Int. Ed.* **2011**, *123*, 1403–1406.
25. Osipova, E.S.; Belkova, N.V.; Epstein, L.M.; Filippov, O.A.; Kirkina, V.A.; Titova, E.M.; Rossin, A.; Peruzzini, M.; Shubina, E.S. Dihydrogen bonding and proton transfer from MH and OH acids to Group 10 metal hydrides [(^tBuPCP)MH][^tBuPCP = $\kappa^3\text{-2,6-(tBu}_2\text{PCH}_2)_2\text{C}_6\text{H}_3$; M = Ni, Pd]. *Eur. J. Inorg. Chem.* **2016**, *2016*, 1415–1424.
26. Eckert, F.; Leito, I.; Kaljurand, I.; Kütt, A.; Klamt, A.; Diedenhofen, M. Prediction of acidity in acetonitrile solution with COSMO-RS. *J. Comput. Chem.* **2009**, *30*, 799–810.
27. Osipova, E.S.; Gulyaeva, E.S.; Kireev, N.V.; Kovalenko, S.A.; Bijani, C.; Canac, Y.; Valyaev, D.A.; Filippov, O.A.; Belkova, N.V.; Shubina, E.S. Fac-to-mer isomerization triggers hydride transfer from Mn (I) complex fac-[(dppm)Mn(CO)₃H]. *Chem. Comm.* **2022**, *58*, 5017–5020.
28. Kaljurand, I.; Kütt, A.; Sooväli, L.; Rodima, T.; Mäemets, V.; Leito, I.; Koppel, I.A. Extension of the self-consistent spectrophotometric basicity scale in acetonitrile to a full span of 28 pKa units: Unification of different basicity scales. *J. Org. Chem.* **2005**, *70*, 1019–1028.
29. Tabassum, S.; Sereida, O.; Reddy, P.V.G.; Wilhelm, R. Hindered Brønsted bases as Lewis base catalysts. *Org. Biomol. Chem.* **2009**, *7*, 4009–4016.
30. Narayanan, B.; Amatore, C.; Kochi, J. Electroreduction of carbonylmanganese (I) cations. Mechanism of ligand substitution and hydride formation via manganese (0) intermediates. *Organometallics.* **1987**, *6*, 129–136.
31. Booth, B.; Haszeldine, R., Metal carbonyl chemistry. Part I. The reactions of phosphorus-containing ligands with hydridopentacarbonylmanganese. *J. Chem. Soc. A* **1966**, 157–160.
32. Danopoulos, A.A.; Pugh, D.; Smith, H.; Saßmannshausen, J. Structural and reactivity studies of “pincer” pyridine dicarbene complexes of Fe0: Experimental and computational comparison of the phosphine and NHC donors. *Chem. Eur. J.* **2009**, *15*, 5491–5502.
33. Zhen, Y.; Feighery, W.G.; Lai, C.K.; Atwood, J.D. Steric and electronic factors that control two-electron processes between metal carbonyl cations and anions. *J. Am. Chem. Soc.* **1989**, *111*, 7832–7837.
34. Mandal, S.K.; Feldman, J.; Orchin, M. A New route to manganese and rhenium carbonyl tetrafluoroborate salts and an improved procedure for preparing their precursor hydrides. *J. Coord. Chem.* **1994**, *33*, 219–221.
35. Chai, J.-D.; Head-Gordon, M. Long-range corrected hybrid density functionals with damped atom–atom dispersion corrections. *Phys. Chem. Chem. Phys.* **2008**, *10*, 6615–6620.
36. Weigend, F.; Ahlrichs, R. Balanced basis sets of split valence, triple zeta valence and quadruple zeta valence quality for H to Rn: Design and assessment of accuracy. *Phys. Chem. Chem. Phys.* **2005**, *7*, 3297–3305.
37. Frisch, M.J.; Trucks, G.W.; Schlegel, H.B.; Scuseria, G.E.; Robb, M.A.; Cheeseman, J.R.; Montgomery, J.J.A.; Vreven, T.; Kudin, K.N.; et al. *Gaussian 09, Revision D.1*; Gaussian, Inc.: Wallingford, CT, USA, 2009.
38. Marenich, A.V.; Cramer, C.J.; Truhlar, D.G. Universal solvation model based on solute electron density and on a continuum model of the solvent defined by the bulk dielectric constant and atomic surface tensions. *J. Phys. Chem. B* **2009**, *113*, 6378–6396.
39. Dolomanov, O.V.; Bourhis, L.J.; Gildea, R.J.; Howard, J.A.; Puschmann, H. OLEX2: A complete structure solution, refinement and analysis program. *J. Appl. Crystallogr.* **2009**, *42*, 339–341.
40. Sheldrick, G.M. SHELXT—Integrated space-group and crystal-structure determination. *Acta Crystallogr. A* **2015**, *71*, 3–8.
41. Sheldrick, G.M. A short history of SHELX. *Acta Crystallogr. A* **2008**, *64*, 112–122.

Disclaimer/Publisher’s Note: The statements, opinions and data contained in all publications are solely those of the individual author(s) and contributor(s) and not of MDPI and/or the editor(s). MDPI and/or the editor(s) disclaim responsibility for any injury to people or property resulting from any ideas, methods, instructions or products referred to in the content.